Microscopy and Microanalysis (2019), 1–10
doi:10.1017/S1431927619015058

Microscopy AND Microanalysis

Original Article

Neutron Autoradiography Combined With UV-C Sensitization: Toward the Intracellular Localization of Boron

Mario A. Gadan[1,2], Rodrigo Lloyd[2,3,4], Gisela Saint Martin[5], María S. Olivera[6], Lucía Policastro[2,3,7] and Agustina M. Portu[2,5,7]*

[1]Department of Instrumentation and Dosimetry, National Atomic Energy Commission (CNEA), Av. General Paz 1499, B1650KNA, San Martín, Buenos Aires, Argentina; [2]Institute of Nanoscience and Nanotechnology (INN), Av. General Paz 1499, B1650KNA, San Martín, Buenos Aires, Argentina; [3]Laboratory of Nanomedicine, CNEA, Av. General Paz 1499, B1650KNA, San Martín, Buenos Aires, Argentina; [4]National Agency for Scientific and Technological Promotion (ANPCyT), Godoy Cruz 2270, C1425FQD, Ciudad Autónoma de Buenos Aires, Argentina; [5]Department of Radiobiology, CNEA, Av. General Paz 1499, B1650KNA, San Martín, Buenos Aires, Argentina; [6]Department of Boron Neutron Capture Therapy, CNEA, Av. General Paz 1499, B1650KNA, San Martín, Buenos Aires, Argentina and [7]National Scientific and Technical Research Council (CONICET), Godoy Cruz 2270, C1425FQD, Ciudad Autónoma de Buenos Aires, Argentina

Abstract

Our group has reported the imprint formation of biological material on polycarbonate nuclear track detectors by UV-C exposure, which is used as an approach to simultaneously visualize cell imprints and nuclear tracks coming from the boron neutron capture reaction. Considering that the cell nucleus has a higher UV-C absorption than the cytoplasm and that hematoxylin preferentially stains the nucleus, we proposed to enhance the contrast between these two main cell structures by hematoxylin staining before UV-C sensitization. In this study, several experiments were performed in order to optimize UV-C exposure parameters and chemical etching conditions for cell imprint formation using the SK-BR-3 breast cancer cell line. The proposed method improves significantly the resolution of the cell imprints. It allows clear differentiation of the nucleus from the rest of the cell, together with nuclear tracks pits. Moreover, it reduces considerably the UV-C exposure time, an important experimental issue. The proposed methodology can be applied to study the boron distribution independently from the chosen cell line and/or boron compounds.

Key words: boron microdistribution, boron neutron capture therapy (BNCT), neutron autoradiography, polycarbonate nuclear track detector, UV-C sensitization

(Received 8 May 2019; revised 10 September 2019; accepted 15 October 2019)

Introduction

Boron neutron capture therapy (BNCT) is a combined radiotherapy modality for the locoregional control of solid tumors. It is based on the administration of a ^{10}B-enriched compound that selectively accumulates in tumor cells and the subsequent neutron irradiation of the region to be treated. In this way, the neutron capture reaction $^{10}B(n,\alpha)^{7}Li$ (BNC), which is highly probable for thermal neutrons, takes place for emitting an α-particle and a recoiling ^{7}Li ion. These charged particles are emitted with high linear energy transfer and short-range in tissue, comparable to cell size (e.g., Moss, 2014). The effectiveness of BNCT depends on the selective accumulation of ^{10}B atoms within the cancer cells, given that the most relevant dose component is due to the disintegration that follows the capture reaction. This represents a radiobiological advantage in comparison to other radiotherapy modalities. Hence, BNCT would make possible the selective damage of infiltrating tumor cells in the healthy tissue, which is a challenge for current radiotherapy.

*Author for correspondence: A. M. Portu, E-mail: agustina.portu@gmail.com

Cite this article: Gadan MA, Lloyd R, Saint Martin G, Olivera MS, Policastro L, Portu AM (2019) Neutron Autoradiography Combined With UV-C Sensitization: Toward the Intracellular Localization of Boron. *Microsc Microanal*. doi:10.1017/S1431927619015058

In this context, the knowledge of ^{10}B atoms localization at the tissue and even the cellular level is essential to evaluate the success probability of the therapy and to understand the radiobiological effects observed after irradiation (Wittig et al., 2008). This information can be provided by the neutron autoradiography technique using nuclear track detectors (NTDs). It is a powerful methodology that correlates ^{10}B spatial microdistribution in a given sample with the damage (nuclear tracks) registered on the detector (e.g., Rosembaum & Armijo, 1967). The use of NTDs (thermal and electrical insulating materials, both organic and inorganic) is based on their ability to permanently preserve the structural alterations produced by the impact of the particles reaching their surface. These latent damages can be amplified by a chemical etching process. The chemical agents act at a higher rate in the region close to the trajectory of the particle (track velocity, V_t) than that in the bulk material (V_b). This fact generates "channels" that constitute the nuclear tracks, which are visible under the optical or electron microscope (Fleischer et al., 1975).

In the case of samples related to BNCT, the products of the BNC reaction give rise to the tracks on the NTD surface. To this end, the detector-biological sample set (spatially correlated) must undergo thermal neutron irradiation at a specific fluence. Afterwards, the biological sample has to be removed in order to perform the chemical etching. The autoradiographic image is

formed by the nuclear tracks and can be recorded in image analysis systems (e.g., an optical microscope). In order to spatially correlate the microdistribution of nuclear tracks to biological structures of interest, the biological sample must be previously photographed using image co-registration techniques.

Our group has extensively explored different approaches of neutron autoradiography at the tissue level using polycarbonate as the NTD. Both qualitative neutron autoradiography (Portu et al., 2013) and quantitative neutron autoradiography (e.g., Portu et al., 2015*a*) have been applied to different biological models for BNCT studies. Based on the work of Amemiya, Konishi and coworkers on poly-allyl-diglycol carbonate (Amemiya et al., 2005; Konishi et al., 2007), our group has also reported the feasibility of obtaining cellular contours (imprints) on polycarbonate by UV-C exposure, employing the same etching procedure used to enlarge nuclear tracks (Portu et al., 2016). Different experiments were carried out in order to establish cell culture conditions on polycarbonate substrates. Furthermore, optimal conditions were set up to simultaneously visualize cell imprints and nuclear tracks coming from the BNC reaction (Portu et al., 2015*b*). On the other hand, a reduction in the nuclear track density (fading) on sensitized polycarbonate foils by UV-C radiation was reported by our group. A decreasing relation between the track density and exposure time to UV-C was observed for ions coming from the BNC reaction (Saint Martin et al., 2017), and it was found that increasing UV-C exposure time enlarges V_b up to saturation.

In this work, we present an improvement in the neutron autoradiography technique combined with the UV-C sensitization of polycarbonate NTD. The aim was to enhance spatial resolution between nuclear tracks and main cell structures or compartments, such as nucleus and cytoplasm. The study was focused on shortening the UV-C irradiation time. Track density loss produced by UV-C exposure could be reduced, achieving the contrast enhancement of cell imprints while preserving nuclear tracks in a single image. In this way, the use of image co-registration methods can be avoided.

Materials and Methods

Cell Lines

Human breast cancer cell lines used in this study included SK-BR-3 and MCF-7. They correspond to HER2+ and luminal A cancer subtypes, respectively (Holliday & Speirs, 2011). The SK-BR-3 cell line was maintained in McCoy's 5A medium (Sigma-Aldrich), while Dulbecco's Modified Eagle Medium/Nutrient Mixture F-12 (Gibco) was used for the MCF-7 cell line. Both media were supplemented with 10% (vol/vol) fetal bovine serum (FBS, Natocor), 1 mM L-glutamine (Biopack), 100 IU/mL penicillin, and 100 µg/mL streptomycin (Sigma-Aldrich). Cells were maintained at 37°C in a 5% (vol/vol) CO_2 humid atmosphere.

Cell Attachment and Fixation

Preliminary studies were performed in order to establish experimental conditions for cell attachment to a polycarbonate detector (Lexan™ 8010, SABIC Innovative Plastics, polished graphic grade). Circular polycarbonate detector foils of 250 µm thickness and diameter compatible with 24-well-plate (p-24) dimensions were sterilized in 70% ETOH 3 h before cell seeding. In order to improve cell attachment, different strategies were addressed. Lexan foils were embedded in phosphate-buffered saline (PBS, Biopack), culture medium, or FBS for 24 h. These foils were washed with PBS and deposited on tissue culture nontreated p-24 wells (Jet Biofil) for subsequent cell seeding. After 24 h, the culture medium was removed, and the cells were washed three times with PBS and fixed with TEM-quality glutaraldehyde (Ted Pella) in 2% PBS for 10 min at low temperature. Finally, the fixation solution was removed and the foils with fixed cells were allowed to dry. As a control of cell growth, cells were also seeded on a p-24 well (standard condition).

Cell Imprints

Considering that the cell nucleus has a higher UV absorption than the cytoplasm and that hematoxylin preferentially stains the nucleus (Giese, 1964), we proposed to enhance the contrast between these two main cell structures by hematoxylin staining before performing UV-C sensitization. We studied the imprint formation using the SK-BR-3 cell line and hematoxylin staining (Biopack) for 5 and 15 min. A control group without hematoxylin was also evaluated.

Fixed cells on the NTD (with or without staining) were irradiated with UV-C at different exposure times: 2, 5, 15, and 30 min and 1, 2, and 6 h. These last two exposure times were included according to previous experiences (Portu et al., 2015*b*). The UV-C irradiation was performed with a 15 W UV lamp with 254 nm wavelength emission (G15T8, General Electric) (Portu et al., 2016). Samples were exposed to a homogeneous field, where the average radiance was 6.1 ± 0.2 mW/cm^2 (radiometer International Light Technologies ILT77). After UV-C exposure, the cells were detached from the detector surface with trypsin-EDTA (Sigma Life Science). Then, a chemical etching was performed using PEW (30 g KOH, 80 g ethyl alcohol, and 90 g of distilled water) as an etchant solution at 70°C for 2 and 4 min.

Visualization of Cell Imprints and Nuclear Tracks

In order to generate α and ^{7}Li tracks in the Lexan foils for simultaneous visualization with cell imprints, cells were seeded under the established conditions. After 24 h, they were incubated with ^{10}B-enriched boronophenylalanine (Interpharma) combined with fructose (Merk) (BPA-f) added to the corresponding culture medium at a final concentration of 30 ppm (mg/L) of ^{10}B during 48 h. The incubation time was chosen to assure enough boron incorporation to set up the technique proposed in this work. Then, the culture medium was removed. The cells were washed three times with PBS and fixed with the previously described process. Samples were irradiated at 10^{12} or 10^{13} cm^{-2} neutron fluences at the RA-3 reactor (Ezeiza Atomic Center, CNEA, Buenos Aires, Argentina). Once neutron irradiation was performed, the same procedures described in *Cell imprints* were carried out.

Effect of UV-C Exposure in Chemical Etching Kinetics

The bulk etch rate, V_b (µm/h), was determined for 2 and 5 min of UV-C exposure of the polycarbonate foils, using the relation in (1) below, from measurements of removed material thickness (H) at different etching times (0.5, 1, 2, 4, 6, 8, and 10 min).

$$H = V_b \cdot t \quad (1)$$

https://doi.org/10.1017/S1431927619015058

Steps were created on the polycarbonate foils by partially covering its surface with epoxy resin before the etching process. Measurements of H (μm) were performed with a surface profiler (KLA-Tencor AlphaStep D-120 Stylus) at the Micro and Nano Technology Department (Constituyentes Atomic Center, CNEA, Buenos Aires, Argentina). The measured values of H were compared with those reported by our group for unexposed foils and for the "30 min UV-C" condition (Saint Martin et al., 2017).

Fading Study

In order to characterize the fading effect on nuclear tracks in autoradiographic images with cell imprints, qualitative and quantitative track density analyses were performed. As a first step, the fading effect was evaluated on images of nuclear tracks without cell imprints. For this purpose, a reference sample with homogeneous boron distribution was chosen. Subsequently, this effect was studied on autoradiographic images with cell imprints. Due to biological variability related to boron incorporation, this condition has an intrinsic heterogeneity in nuclear tracks distribution that has to be taken into account for further analysis.

Homogeneous Track Distribution

A ^{10}B implant in silicon standard NIST 2137 (National Institute of Standards & Technology), in contact with polycarbonate foils, was exposed to a neutron fluence of 10^{12} cm^{-2}. This fluence is low enough to avoid nuclear tracks overlapping that could jeopardize individual counting. Following neutron irradiation, foils were exposed to UV-C radiation for 5 or 30 min with subsequent chemical etching. As a reference, these foils were compared to the no UV-C exposure condition. Finally, microscopic photographs of the nuclear tracks were obtained and analyzed as detailed in *Imaging and Analysis*.

Heterogeneous Track Distribution

Several experiments were performed employing SK-BR-3 cells incubated with BPA-f. The procedure previously described in the section *Visualization of cell imprints and nuclear tracks* was applied. After neutron irradiation, the cells fixed on Lexan foils were subjected to different conditions (Table 1).

The same etching process was applied to all foils, and photomicrographs were acquired for the qualitative and quantitative analysis of track density.

Imaging and Analysis

Photomicrographs were obtained with an optical microscope (Olympus BX51), coupled to a CCD camera (Olympus DP70). Light conditions were set in order to obtain best quality and reproducible images.

In order to quantify the track density from autoradiographic images, nuclear tracks must be recognized and counted. An image analysis process was carried out using the software Image Pro Premier™ 9.2 (Media Cybernetics). Image segmentation based on thresholding was firstly applied to each grayscale image. Then, a learning classification method based on manually selected reference objects was applied in order to differentiate nuclear track pits from other objects obtained in the segmentation process. Multiple parameters that could be relevant in the distinction of nuclear tracks had been previously studied, including area, circularity, and aspect ratio, were used for training the algorithm. The training was performed for measuring these parameters in several objects manually selected by the user. This process was validated by comparing results with manual counting.

Table 1. Hematoxylin Staining and UV-C Irradiation Conditions on Boron-Loaded Cells Fixed on Lexan Foils.

Condition#	Hematoxylin	UV-C
1	No	No
2	No	Yes/5 min
3	Yes/15 min	Yes/5 min
4	Yes/15 min	Yes/30 min

Results

In order to guarantee cell adhesion on polycarbonate, we first tested different pretreatment conditions. The PBS condition was chosen for pretreatment, as it exhibited a negligible effect on cell attachment and growth or morphology when compared to control samples (cells seeded in p-24 well at standard conditions). Other strategies resulted in appreciable cell death or heterogeneous growth. The fixation protocol achieved good maintenance and quality of the cell structure.

After cell attachment and fixation protocols were established, cell imprint formation experiments using hematoxylin staining were performed. In Figure 1, the effect of varying both etching and UV-C exposure times using hematoxylin staining can be observed. The first column shows the cell culture stained with hematoxylin for 5 min before UV-C exposure. The other two columns show the cell imprints of the same region depicted in the first column at different etching times: 2 and 4 min, respectively. Together with etching time variation, the pictures corresponding to UV-C exposure times are presented in the different rows: 15, 30, 60, and 120 min.

The use of hematoxylin before UV-C irradiation allowed the cell nucleus to be clearly distinguished from the rest of the cell. The imprints reproduce the findings in the original stained cell images, such as cells with more than one nucleus. Increasing the etching time from 2 to 4 min resulted in contrast enhancement, along with recording "cleaner" images (fewer superficial artifacts) on Lexan foils. As it is well known, a longer etching time produces a larger nuclear track size, making nuclear tracks better distinguishable from cellular imprints (see ahead in this section). Regarding UV-C irradiation, as exposure time increases, especially 30 min or longer, a more degraded cellular imprint can be observed. This could compromise the ability to highlight cellular structures. Moreover, diminishing exposure time is crucial for track visualization.

Taking into account the preceding results, irradiation times of 2, 5, and 15 min were then studied by increasing the staining time to 15 min while fixing the etching time at 4 min. As control samples, a set of Lexan foils were exposed to UV-C radiation without previous hematoxylin staining. As it was determined in our previous work (Portu et al., 2015*b*), cell structures absorb UV-C radiation at different levels, generating reliefs on the etched detector's surface. In the first column of Figure 2, it is noteworthy that cellular imprints are formed from the UV-C absorption of each cellular structure (focusing on the nucleus and the cytoplasm). In addition, by setting the staining time to 15 min, it can be noticed that the cellular structures in the imprints have greater contrast

https://doi.org/10.1017/S1431927619015058

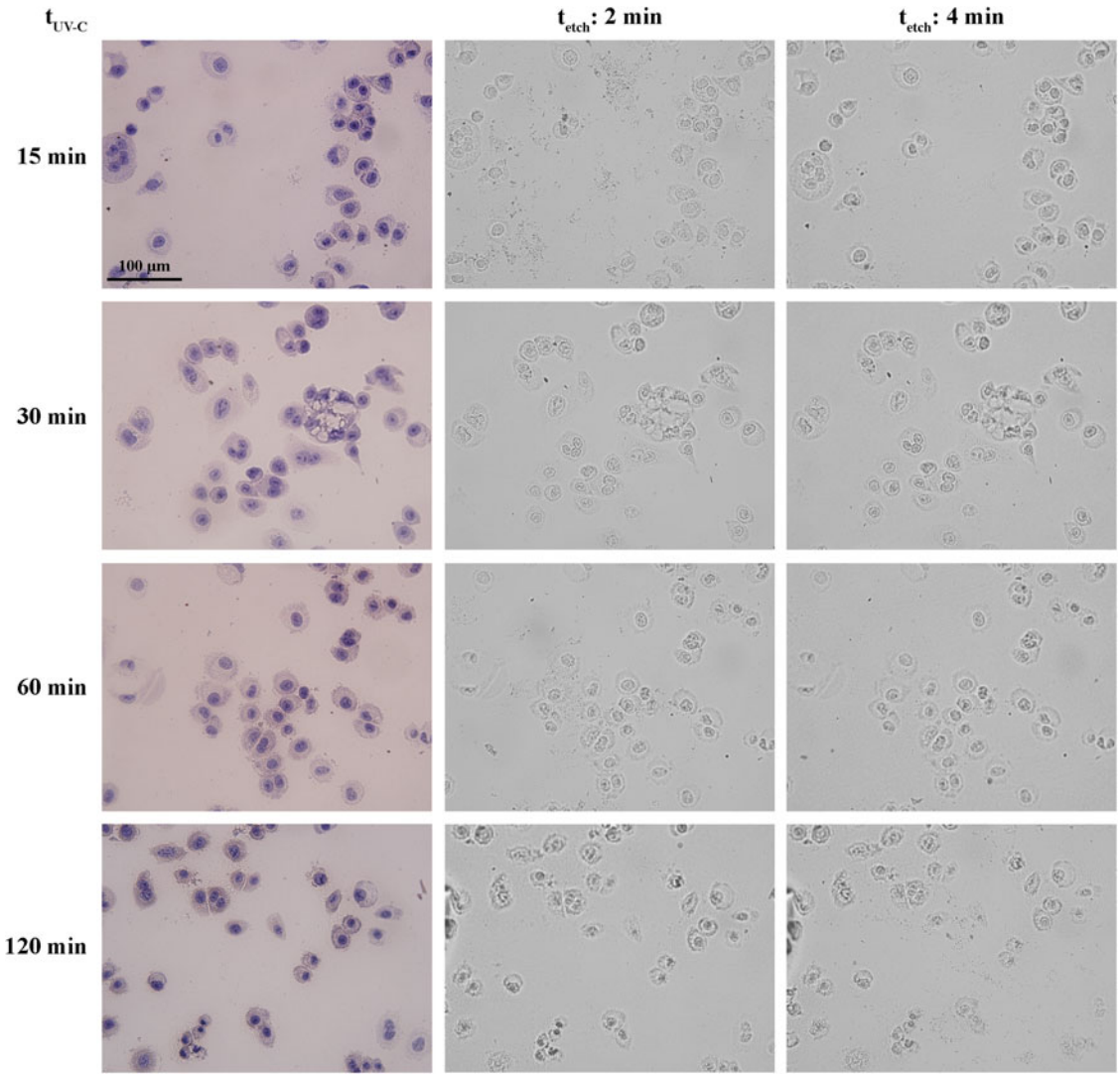

Fig. 1. SK-BR-3 cell imprints obtained with 5 min of hematoxylin staining at different UV-C exposure (t_{UVC}) and etching times (t_{etch}).

for all exposure times. The results obtained for 5 and 15 min presented no significant difference in terms of cellular compartment identification for the proposed analysis. Looking forward to reduce track fading by lowering the exposure time, 15 min of UV-C was discarded. On the other hand, though cellular imprints generated at 2 min exposure could be acceptable, the image contrast of cellular imprints at the exposure time of 5 min seems to be optimal for a clear identification of structures.

Once the parameters to generate cell imprints were established, experiments assessing the simultaneous visualization of nuclear tracks and cellular structures were performed. In Figure 3, the hematoxylin staining can be appreciated, along with the corresponding cell imprints and nuclear tracks images of the same region on the SK-BR-3 cell culture. It must be emphasized that the hematoxylin staining image is shown just to stress the correspondence between the cell imprint image and the original sample. In further analyses, this image would not be necessary. It can be observed that the visualization of tracks or cell imprint can be achieved just with a slight change in the microscope focus. This is related to the fact that both damages occur at different depths in the NTD material structure.

The next step consisted of studying the effect of UV-C on chemical etching kinetics. The V_b was determined from measurements of H for different UV-C and etching times. These results are presented in Figure 4. Higher H values (thus, V_b) were observed for all UV-C conditions, in comparison with unexposed foils. Indeed, the 30 min values were found to be remarkably higher than the other UV-C conditions for all etching times. Nevertheless, considerable differences were also obtained between results corresponding to 2 and 5 min of UV-C. The calculated values of V_b can be observed in Table 2.

In order to depict the fading effect on nuclear tracks from the BNC reaction, the results from the neutron irradiation of the ^{10}B NIST standard in contact with Lexan foils and subsequent exposure to UV-C are shown in Figures 5 and 6. When compared to the control sample (no UV-C exposure), the fading effect is appreciable at 5 and 30 min of UV-C exposure. A quantitative analysis performed on images like those presented in Figure 5 for each case revealed a reduction to a relative track density of (52 ± 4) and (25 ± 2)%, respectively, as shown in Figure 6. Fading is appreciable not only in the track density loss but also in the quality of the track etched pits; as it can be seen from

https://doi.org/10.1017/S1431927619015058

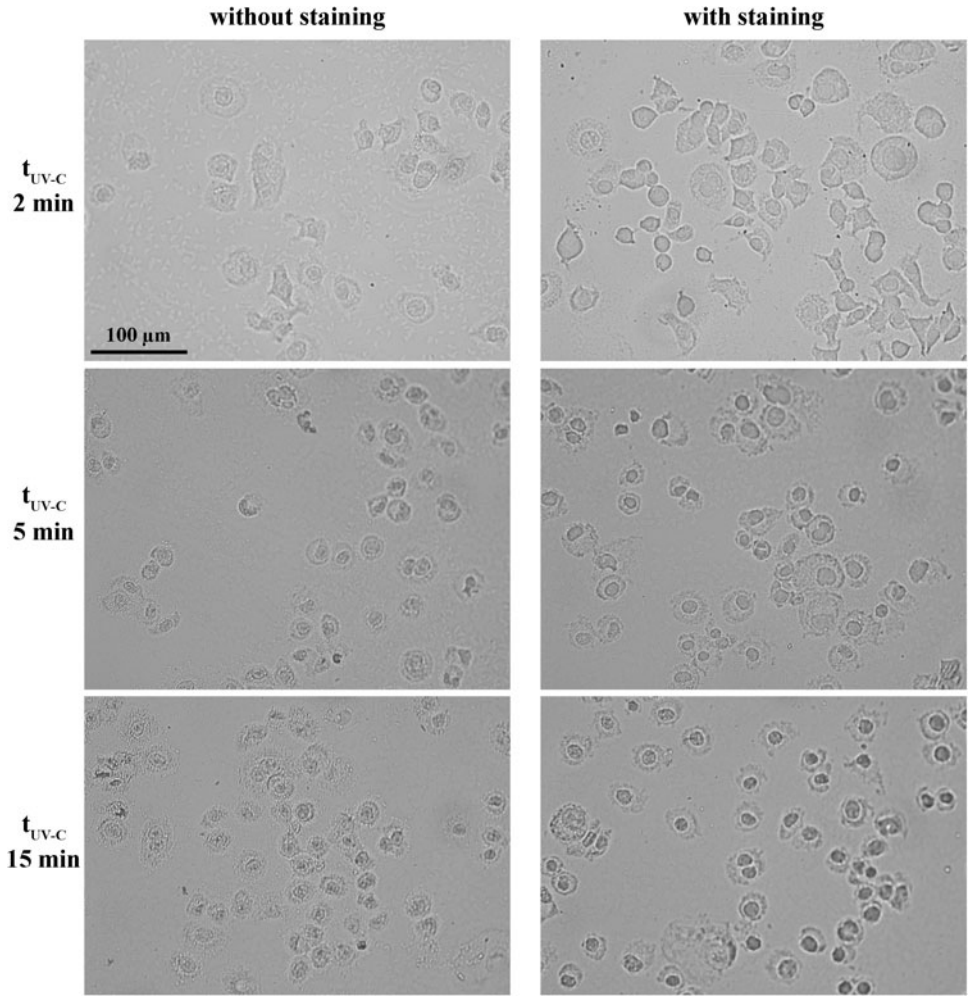

Fig. 2. Comparison of SK-BR-3 cell imprints obtained without or with 15 min hematoxylin staining at different UV-C exposure (t_{UVC}) and a fixed etching time (4 min).

Figure 5 the contrast of tracks (having no clear borders) is degraded with respect to control sample image.

In comparison to fading analysis performed on the NIST standard, where only nuclear tracks form the autoradiographic image, the study of cell imprints is more complex. In these images, it is mandatory to distinguish between objects classified as track pits coming from the BNC reaction and objects that are related with cell imprint structures.

In Figures 7 and 8, it is shown how the object classification learning algorithm worked for samples with nuclear tracks coming from the BNC reaction taking place in cells. The presence of ^{10}B atoms inside the cells can be recognized by the clustered pattern in which nuclear tracks are presented in both images without and with cell imprints (Figs. 7, 8, respectively). As it can be appreciated, blue objects were classified as "nuclear tracks", while green objects were classified as "other objects." These last ones were not considered for track density measurement.

Taking into account Table 1, different conditions were studied. In Figure 9, track density values for 5 min of UV-C (conditions #3 and #2) relative to no UV-C exposure are shown (condition #1 is the reference for this analysis). A loss of track density can be observed regardless the use of hematoxylin staining.

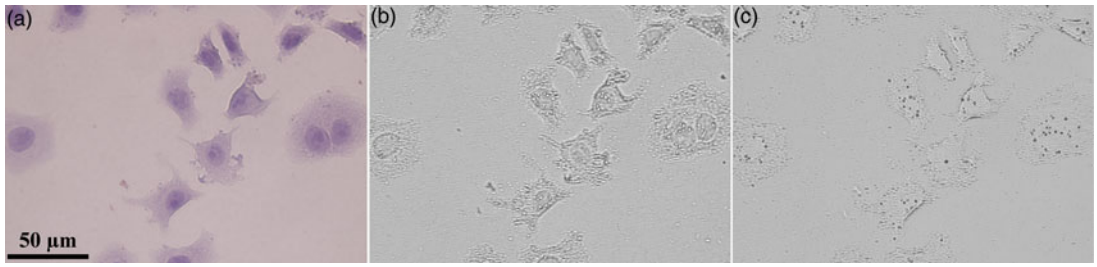

Fig. 3. SK-BR-3 cells cultured on Lexan and stained with hematoxylin (**a**) and their corresponding images of imprints (**b**) and nuclear tracks (**c**).

https://doi.org/10.1017/S1431927619015058

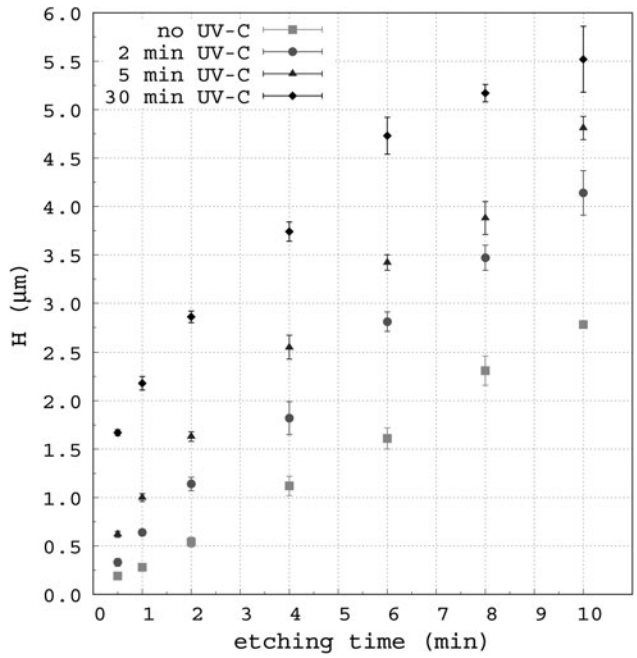

Fig. 4. Removed material thickness (H) for different UV-C and etching times.

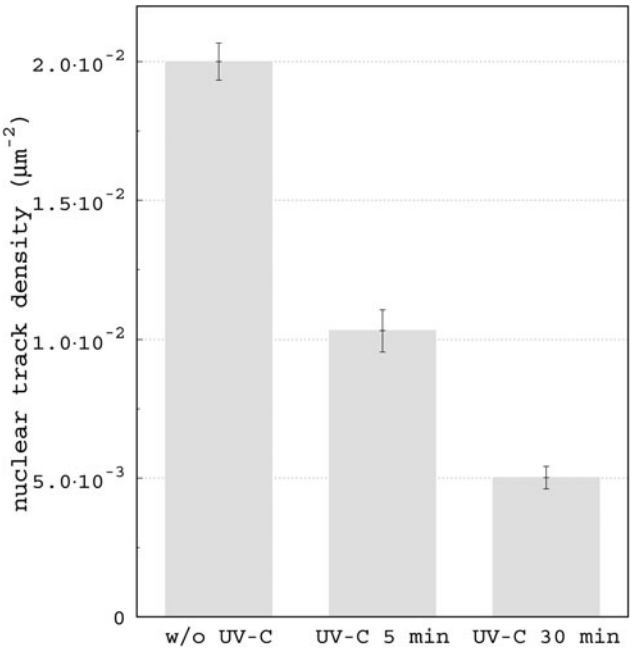

Fig. 6. Fading effect in the nuclear track density (μm^{-2}) in images from the NIST standard, exposed to different UV-C exposure times: no UV-C, UV-C for 5 min, and UV-C for 30 min. The results are presented as average ±1 SD.

Table 2. Average V_b Values for Different UV-C Exposure Times.

UV-C time	V_b (μm/min)
0 (no UV-C)	0.28 ± 0.03
2 min	0.45 ± 0.04
5 min	0.64 ± 0.03
30 min	0.93 ± 0.02

V_b values were calculated for 4 min etching time.

Furthermore, this loss is greater under the no hematoxylin staining condition (about 40% without staining versus 18% with staining). It should be noted that the dispersion found in track density measurements for these samples (which is about 20%) is not related to the measurement method but to the biological variability associated with cell seeding and boron uptake. Also, the UV-C exposure time of 30 min (condition #4) was qualitatively compared to the 5 min exposure (condition #3), and the loss in track density is remarkable, nuclear tracks are smaller, and the contrast is poorer, as shown in Figure 10. No further quantitative analysis was necessary to demonstrate the considerable fading effect observed for 30 min.

Discussion

In the frame of the Argentinean Boron Neutron Capture Therapy Project at the National Atomic Energy Commission (CNEA), a research line, aimed to study the feasibility of applying BNCT to the treatment of locoregional recurrences of the HER-2 breast cancer subtype, is under development (Gadan et al., 2015). The strategy considers the design and use of immunoliposomes as boron carrier nanovehicles to target HER-2-overexpressing cells as a paradigm case study. In this context, neutron autoradiography combined with UV-C sensitization would allow the optimization of the study of boron nanovehicle delivery performance.

In order to establish experimental conditions for this application, SK-BR-3 and MCF-7 breast cancer cell lines were chosen in

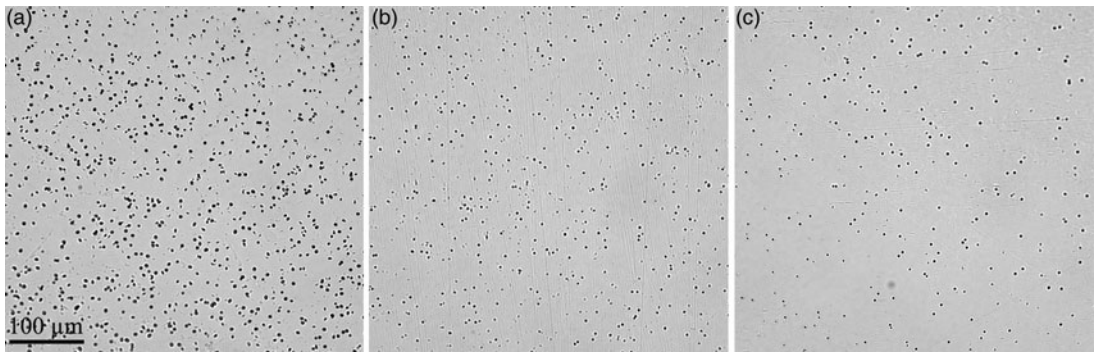

Fig. 5. Nuclear tracks coming from a NIST standard with (**a**) no UV-C exposure, (**b**) 5 min of UV-C, and (**c**) 30 min of UV-C.

https://doi.org/10.1017/S1431927619015058

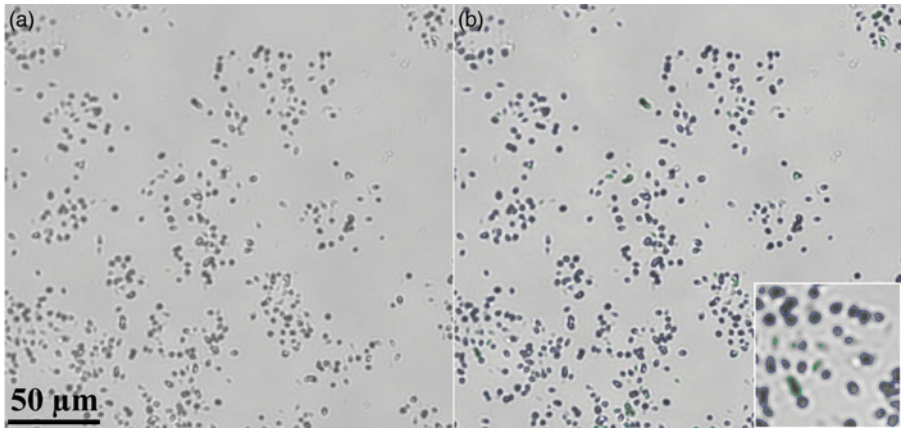

Fig. 7. (**a**) Nuclear tracks coming from the BNC reaction taking place in ^{10}B atoms in SK-BR-3 cells. (**b**) Object classification by the learning algorithm: blue objects correspond to "nuclear tracks", while green objects were classified as "other objects".

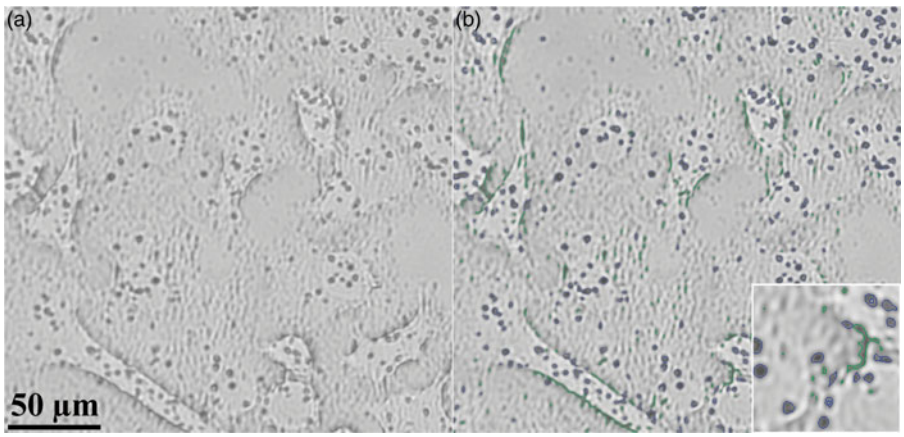

Fig. 8. (**a**) Nuclear tracks coming from the BNC reaction taking place in ^{10}B atoms in SK-BR-3 cells. The fixed cells on polycarbonate were stained for 15 min, exposed to UV-C radiation for 5 min and etched for 4 min. (**b**) Object detection by the learning algorithm: blue objects correspond to "nuclear tracks", while green objects were classified as "other objects".

the current study. Cell seeding and growth conditions on polycarbonate detectors were successfully established for the SK-BR-3 breast cancer cell line. The described protocol could vary when working with other cell lines. Indeed, in previous works performed with melanoma cell lines, a pretreatment with the culture medium for 24 h was necessary to obtain adequate cell distribution on Lexan (Portu et al., 2015*b*; Rossini et al., 2015).

The established protocol was also applied in the MCF-7 breast cancer cell line, as a way to test our set up on another cell line of interest. As it is shown in Figure 11, not only good quality cell growth but also clearly defined imprints and nuclear tracks were obtained. This is a relevant issue given the potential application of this technique for boron compound performance assessment. Nevertheless, the protocol should be revised when changing the cell line.

It can be observed that cell imprint formation is related to nonuniform damages over the polycarbonate detector due to differences in the UV-C absorption by diverse cell structures, the cell nucleus has a higher absorption than the cytoplasm. The use of hematoxylin highlights this effect due to cell nucleus preferential staining and consequently acting as an UV-C "protector". Then, only 5 min of UV-C exposure is enough to obtain high-quality imprint images when hematoxylin is previously used. This fact represents a considerable reduction of irradiation time, in comparison with the 6 h UV-C exposure applied in previous studies (Portu et al., 2015*b*).

Moreover, the "protective" effect of hematoxylin can be seen from images in Figure 12. SK-BR-3 cells fixed to polycarbonate detectors were stained for 5 min with hematoxylin and exposed to UV-C for 2 or 6 h. Finally, the detector was etched for 2 min. At 2 h of UV-C exposure, it is possible to distinguish the cellular nucleus and the cytoplasm. Although the cytoplasm contours are poorly defined, it is possible to differentiate the cells from each other. Even the regions of higher contrast within the nuclei (e.g., the nucleoli) can be observed, as they have a greater absorption of hematoxylin. On the other hand at 6 h UV-C exposure, it was observed that the cellular structures less stained with hematoxylin disappeared, while the structures with greater staining (nuclei) remained with sharp contours.

Regarding the visualization of cell imprints together with nuclear tracks, well-contrasted images were obtained for all the studied conditions, except for 2 min of UV-C exposure time. Moreover, the best quality images were observed for UV-C irradiation times ranging from 5 min up to 30 min. In that range, the

https://doi.org/10.1017/S1431927619015058

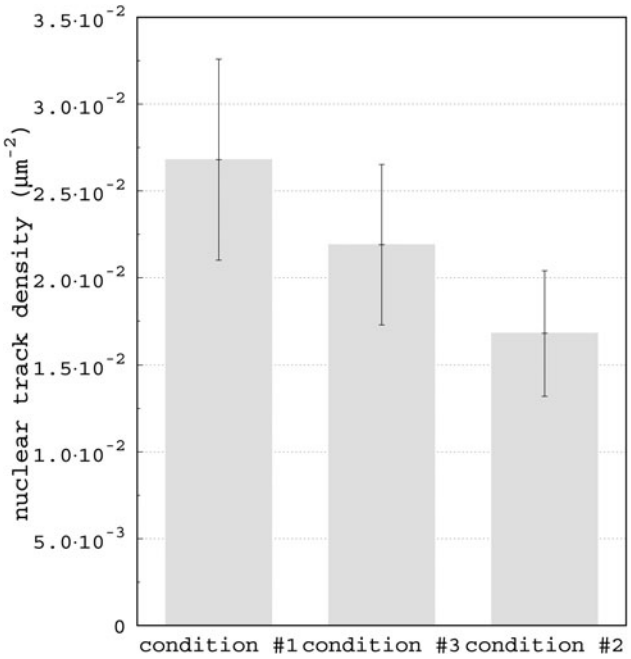

Fig. 9. Nuclear track density values corresponding to the conditions presented in Table 1. The cells fixed on polycarbonate were subjected to different conditions (refer to Table 1): #1 (no UV-C exposure), #2 (exposed to UV-C radiation for 5 min), #3 (staining for 15 min and UV-C exposure for 5 min). The results are presented as average ±1 SD.

imprints exhibit no appreciable differences. For exposure times larger than 30 min, a degradation of the contours and a consequent loss of contrast were observed.

Given that a fading effect on nuclear tracks was found to be related to UV-C irradiation time (Saint Martin et al., 2017), the shortest exposure time was chosen to diminish this effect without compromising cell imprints quality. Indeed, track density decrease and track quality loss were observed for 30 min of UV-C exposure in Figure 10. This is an important issue and must be taken into account when trying to quantify the track density from unknown samples after UV-C sensitization.

Reducing the UV-C exposure time has a direct effect on the nuclear track density, as was observed from the NIST standard analysis. Nevertheless, when no biological material protects the detector, almost half of the nuclear tracks are lost with 5 min of UV-C exposure. When a biological matrix (e.g., fixed cells w/ out staining) is put in contact with the detector, a slight increment on the relative track density can be observed. Moreover, the protective effect of hematoxylin has an impact on track density; when staining is performed before the irradiation, around 75% of nuclear tracks are conserved (Fig. 9). However, due to the biological variability (different boron uptake from cell to cell, among other effects), this value cannot be considered to be a constant. Figure 13 shows the track density measurement under the staining condition and 5 min UV-C exposure, relative to no UV-C exposure. There is a similar track density loss in the different samples within the analyzed uncertainties.

In this work, we established the parameters to achieve high contrast cell imprints together with nuclear tracks. The ability to distinguish between cell compartments (nucleus and cytoplasm) is of great importance to study the microdosimetry, as which the distribution of nuclear track in the cell should be known. In that case, individual nuclear track counting would be required in order to perform an accurate track density determination among cell compartments. Further analysis including track

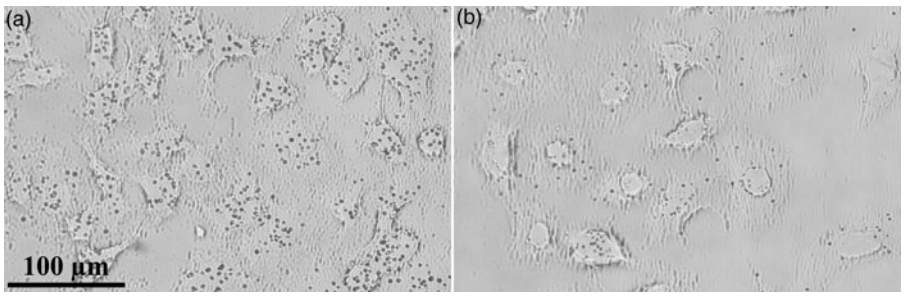

Fig. 10. Qualitative comparison of the nuclear track density when the fixed cells on polycarbonate were stained and then irradiated with UV-C for (**a**) 5 min and (**b**) 30 min.

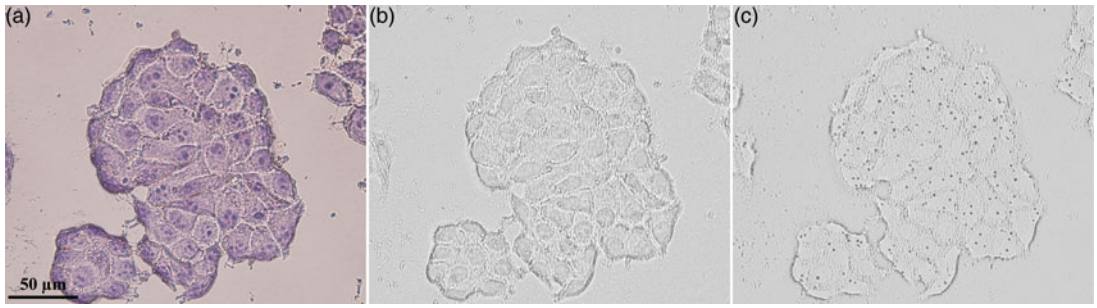

Fig. 11. MCF-7 cells cultured on Lexan and stained with hematoxylin (**a**) and its corresponding images of imprints (**b**) and nuclear tracks (**c**).

https://doi.org/10.1017/S1431927619015058

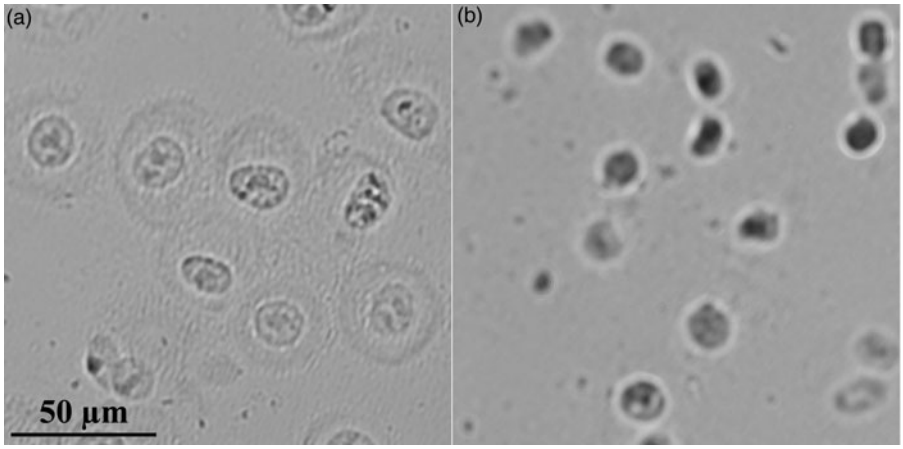

Fig. 12. Cell imprint formation with 5 min of hematoxylin staining and UV-C exposure times of (**a**) 2 h and (**b**) 6 h. Etching time: 2 min.

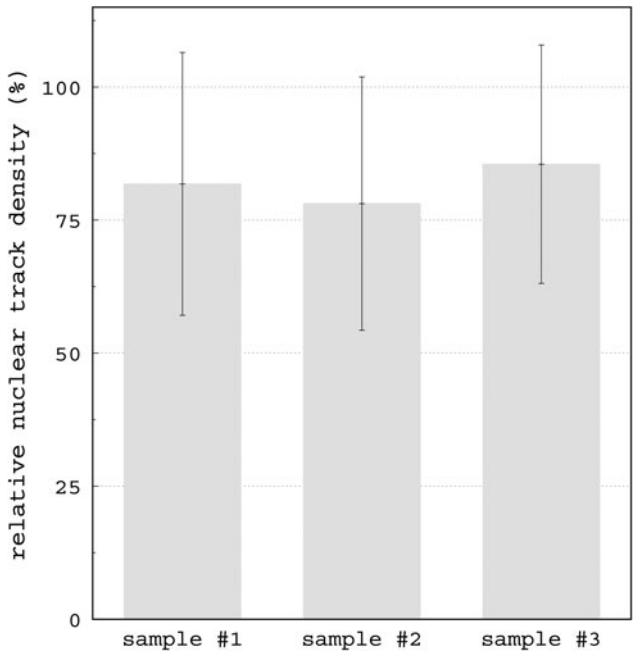

Fig. 13. Different samples exposed to the optimal condition: 15 min of hematoxylin staining, 5 min of UV-C, and 4 min of etching. The results are presented as average ±1 SD.

density measurement per cell compartment could give rise to more precise results. This study is beyond the scope of this work, but it could be achieved with the established technique.

Conclusions

Through the different experiments presented in this work, a protocol was established to obtain high-resolution autoradiographic images of cellular imprints together with nuclear tracks coming from the BNC reaction, without the use of co-registration image techniques. Moreover, applying this method does not require special equipment or imaging acquisition devices.

Complementarily, we were able to dramatically decrease the UV-C exposure time, thus reducing the fading effect. We also characterized this effect for the first time in autoradiographic images coming from biological samples.

This method is a tool that can be applied to different cell lines to study and compare different boron compounds according to their microdistribution. Furthermore, this technique could have a crucial impact in BNCT microdosimetry calculations where spatial microdistribution is required.

Acknowledgments. The authors gratefully acknowledge Dr. Patricia Elizalde and colleagues of Molecular Mechanisms of Carcinogenesis and Molecular Endocrinology of the Institute of Biology and Experimental Medicine (IBYME) for providing the SK-BR-3 cell line. They also thank to Lic. Silvia Thorp, Dr. Emiliano Pozzi, and Mrs. Paula Curotto for the irradiations at the thermal column of the RA-3 reactor (Ezeiza Atomic Center, CNEA, Buenos Aires, Argentina). The authors are grateful with the staff of the Laboratory of Nanomedicine for their assistance and fruitful discussion and with the technical staff of the Micro and Nano Technology Department of the Constituyentes Atomic Center (CNEA, Buenos Aires, Argentina) for their assistance with the profile measurements.

Financial support. This study was partially supported by a grant from the National Agency for Scientific and Technological Promotion (PICT 2016-0407, ANPCyT).

References

Amemiya K, Takahashi H, Kajimoto Y, Nakazawa M, Yanagie H, Hisa T, Eriguchi M, Nakagawa Y, Majima T, Kageji T, Sakurai Y, Kobayashi T, Konishi T, Hieda K, Yasuda N & Ogura K (2005). High-resolution nuclear track mapping in detailed cellular histology using CR-39 with the contact microscopy technique. *Radiat Meas* **40**, 283–288.

Fleischer RL, Price P & Walker RM (1975). *Nuclear Tracks in Solids*. Berkeley, CA, USA: University of California Press.

Gadan MA, González SJ, Batalla M, Olivera MS, Policastro L & Sztejnberg ML (2015). Application of BNCT to the treatment of HER2+ breast cancer recurrences: Research and developments in Argentina. *Appl Radiat Isot* **104**, 155–159.

Giese AC (1964). *Photophisiology Volume 2: Action of Light on Animals and Microorganism; Photobiochemical Mechanism; Bioluminescence*. New York, NY, USA: Academic Press.

Holliday DL & Speirs V (2011). Choosing the right cell line for breast cancer research. *Breast Cancer Res* **13**, 125.

Konishi T, Amemiya K, Natsume T, Takeyasu A, Yasuda N, Furusawa Y & Hieda K (2007). A new method for the simultaneous detection of mammalian cells and ion tracks on a surface of CR 39. *J Radiat Res* **48**, 255–261.

Moss RL (2014). Critical review, with an optimistic outlook, on boron neutron capture therapy (BNCT). *Appl Radiat Isot* **88**, 2–11.

Portu A, Carpano M, Dagrosa A, Cabrini R & Saint Martin G (2013). Qualitative autoradiography with polycarbonate foils enables histological and track analyses on the same section. *Biotech Histochem* **88**, 217–221.

https://doi.org/10.1017/S1431927619015058

Portu A, Molinari AJ, Thorp SI, Pozzi ECC, Curotto P, Schwint AE & Saint Martin G (2015*a*). Neutron autoradiography to study boron compound microdistribution in an oral cancer model. *Int J Radiat Biol* **91**(4), 329–335.

Portu A, Rossini A, Gadan MA, Bernaola OA, Thorp SI, Curotto P, Pozzi ECC, Cabrini RL & Saint Martin G (2016). Experimental set up for the irradiation of biological samples and nuclear track detectors with UV C. *Rep Pract Oncol Radiother* **21**, 129–134.

Portu A, Rossini A, Thorp SI, Curotto P, Pozzi ECC, Granell P, Gomar F, Cabrini RL & Saint Martin G (2015*b*). Simultaneous observation of cells and nuclear tracks from the boron neutron capture reaction by UV-C sensitization of polycarbonate. *Microsc Microanal* **21**, 796–804.

Rosembaum HS & Armijo J (1967). Fission track etching as a metallographic tool. *J Nucl Mater Manage* **22**, 115–116.

Rossini A, Dagrosa MA, Portu A, Saint Martin G, Thorp S, Casal M, Navarro A, Juvenal GJ & Pisarev MA (2015). Assessment of biological effectiveness of boron neutron capture therapy in primary and metastatic melanoma cell lines. *Int J Radiat Biol* **91**(1), 81–89.

Saint Martin G, Portu A, Ibarra ML & Alurralde M (2017). UV-C light radiation effect on nuclear tracks of different ions in polycarbonate. *27th International Conference on Nuclear Tracks and Radiation Measurements (ICNTRM 2017)*, Strasbourg, France.

Wittig A, Michel J, Moss RL, Stecher-Rasmussen F, Arlinghaus HF, Bendel P, Mauri PL, Altieri S, Hilger R, Salvadori PA, Menichetti L, Zamenhof R & Sauerwein WA (2008). Boron analysis and boron imaging in biological materials for boron neutron capture therapy (BNCT). *Crit Rev Oncol Hematol* **68**(1), 66–90.

https://doi.org/10.1017/S1431927619015058